A note on the variation of vibrational temperature along a nozzle

By J. L. STOLLERY AND J. E. SMITH†
Department of Aeronautics, Imperial College, University of London

(Received 21 October 1961)

Vibrational relaxation effects are examined for hypersonic nozzle air flows. A simple method of estimating the distribution of vibrational temperature along a nozzle is described and higher-order approximations discussed. Results are presented for hyperbolic axisymmetric nozzles with reservoir conditions $1000 \leqslant p_0 \leqslant 4000$ p.s.i.a., $1000 \leqslant T_0 \leqslant 3000$ °K. Vibrational freezing is shown to occur and to cause significant changes in the nozzle exit flow conditions.

1. Introduction

The vibrational relaxation times for air expanding through a hypersonic nozzle can be long enough to cause large departures of the vibrational temperature from the equilibrium value. The energy stored in the vibrational mode is relatively small, however, and it therefore seemed unlikely that vibrational non-equilibrium would cause significant changes either in the nozzle flow properties, or in the flow pattern around bodies placed in the stream. For this reason, the problem has merited less attention than that devoted to the effects of dissociation, ionization and chemical reaction.

The authors' interest in vibrational temperature springs from attempts to measure stagnation temperatures in the working section of an intermittent, hypersonic wind tunnel using the Sodium Line Reversal method (Stollery 1961). For a diatomic gas, there is evidence (Clouston, Gaydon & Glass 1958) to suggest that the sodium electronic excitation temperature (which the S.L.R. method measures) 'follows' the vibrational temperature of the gas. The difference between the vibrational and equilibrium temperature is therefore needed to correct the measured values.

2. Method of calculation

The ideal vibrating gas

Following earlier work, for example, on sound dispersion, the appropriate model of a real vibrating gas has been set out by Wood & Kirkwood (1957) and used by Johannesen (1961) and Sedney (1961) in studies behind plane and oblique shock waves, respectively. Briefly the degrees of freedom of the gas are grouped into the active and the inert. Local thermodynamic equilibrium is assumed to exist within these two groups but not between them. For the active group, the perfect gas equation of state is assumed to apply

$$p = \rho R T_a, \tag{1}$$

† Now with the Northern Research and Engineering Corporation.

where p, ρ, T are the pressure, density and temperature. R is the gas constant and the suffices used in this note are given below.

- a the active degrees of freedom (i.e. translation and rotation here);
- e nozzle exit conditions;
- i the inert degrees of freedom (i.e. vibration here);
- o reservoir or stagnation conditions;
- $*$ nozzle throat properties;
- F frozen;
- 1 conditions just ahead of blunt body bow shock wave (§ 6).

The change of entropy dS_a is given by

$$dS_a = Cp_a(dT_a/T_a) - R(dp/p), \tag{2}$$

where Cp is the specific heat at constant pressure. The inert group is assumed to be specified by its temperature T_i so that

$$dS_i = d\sigma/T_i, \tag{3}$$

where $\sigma(T_i)$ is the vibrational energy. The total entropy change dS, is

$$dS = dS_a + dS_i.$$

The enthalpy h becomes

$$h = Cp_a T_a + \sigma(T_i). \tag{4}$$

The vibrational internal energy (σ) for air has been calculated using the harmonic oscillator model and a composition of 20 % oxygen and 80 % nitrogen.

Such a calculation is preferable to subtracting $7/2RT$ from tabulated values of enthalpy (e.g. Hilsenrath *et al.* 1955) since these contain a contribution from other low-lying electronic states of O_2. Thus if the $7/2RT$ for translation and rotation were subtracted, the remainder would not be due solely to the vibrational contribution.

The relevant values are given in table 1.

T °K	Cal./mol. air	T °K	Cal./mol. air
400	5·05	1800	1314
600	39·9	2000	1634
800	134	2200	1982
1000	289	2400	2287
1200	495	2600	2633
1400	740	2800	3001
1600	1018	3000	3345

TABLE 1. Vibrational energy in air.

The rate equation used

$$d\sigma/dx = (\bar{\sigma} - \sigma)/L, \tag{5}$$

is the linear form suggested by Bethe & Teller (1940). The axial co-ordinate x has its origin at the nozzle throat and is positive downstream. $\bar{\sigma}$ is the value that σ would take if equilibrium existed at the temperature T_a. L, the relaxation distance, is the velocity v multiplied by the relaxation time τ. This form of the

rate equation, strictly valid for a system of harmonic oscillators, is a reasonable approximation provided that departures from equilibrium are small. It is used here because it is simple, and no better suggestion backed by either theory or experiment is available.

The vibrational relaxation times for air have been taken from the curve shown in figure 1. This curve passes through the experimental data of Gaydon & Hurle (1960) and is faired towards the experimental data for nitrogen at the lower

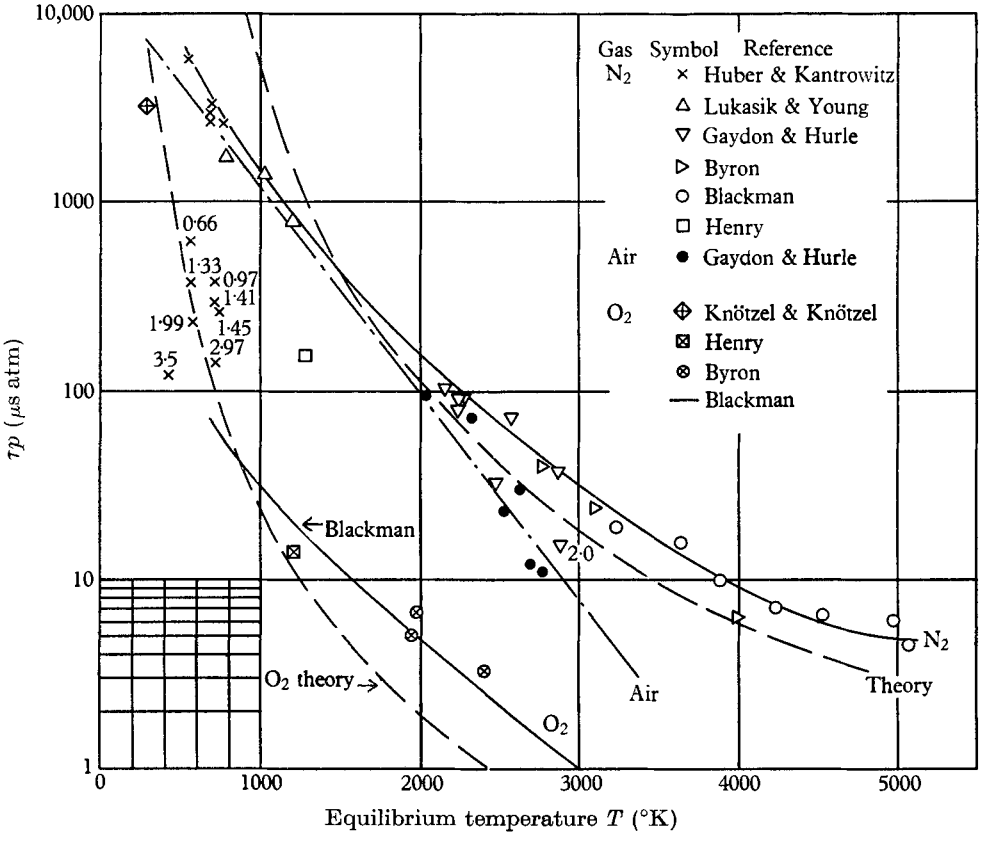

FIGURE 1. Data on vibrational relaxation times for N_2, O_2 and air. (Numbers at the side of the experimental points indicate the percentage of H_2O present in the gas.)

temperatures. This seems reasonable on the grounds that (i) the data for air exhibit this trend, (ii) 80 % of the molecules in air are nitrogen.

Figure 1 contains all the reliable experimental data on N_2, O_2 and air that the authors could find and compares them with the calculations of Dickens & Ripamonti (1961) using the general method of Tanczos (1956). The agreement is reasonable. Apart from emphasizing the dearth of air data, particularly at the lower temperatures, the figure highlights the large differences that impurities make to the measured relaxation times for nitrogen. An excellent critical survey of the experimental data is given in chapter 5 of the book by Cottrell & McCoubrey (1961).

Considering all the information currently available, the curve for air used in the present work seems sensible but necessarily provisional.

Quasi-one-dimensional flow equations

The frictionless adiabatic flow of a vibrating gas passing with velocity $v(x)$ through a nozzle of slowly varying cross-section $A(x)$ may be described by the usual equations of continuity, momentum and energy

$$\rho A v = \text{const.} = \dot{m}, \tag{6}$$

$$-\rho v(dv/dx) = dp/dx, \tag{7}$$

$$h + \tfrac{1}{2}v^2 = \text{const.} = h_0, \tag{8}$$

where the enthalpy $h = Cp_a T_a + \sigma$ and $h_0 = Cp_a(T_a)_0 + \bar{\sigma}_0$. These together with the rate equation (5) and equation of state (1) completely describe the gas.

The equations may be solved for given initial conditions and nozzle geometry by writing them in differential form and employing a numerical step-by-step process. This is extremely laborious and a sample calculation showed no significant difference, in the vibrational temperature, from the simpler method suggested below.

A simple approximation

The vibrational energy, as a percentage of the total internal energy is 4% at 1000 °K and 10% at 2000 °K, so one expects that departures from isentropy, and differences between the local equilibrium temperature T and the local translational temperature T_a, will at most be of similar magnitude. For a first approximation we may assume isentropic perfect gas flow to find the local values of p, v, T_a along the nozzle and hence the values of $\bar{\sigma}(x)$ and $\tau(x)$.

Equation (5) may be written in the form

$$\frac{\sigma_{n+1} - \sigma_n}{\Delta x} = \frac{\tfrac{1}{2}(\bar{\sigma}_{n+1} + \bar{\sigma}_n) - \tfrac{1}{2}(\sigma_{n+1} + \sigma_n)}{\tfrac{1}{2}(L_{n+1} + L_n)}. \tag{5a}$$

A plot of $\bar{\sigma}$ and L against x helps in selecting suitable intervals Δx when using the step-by-step process suggested by equation (5*a*) above. The procedure starts by assuming equilibrium at nozzle entry, i.e. $\sigma_1 = \bar{\sigma}_1$ hence σ_2 and σ_n.

It is now possible to use this first approximation to $\sigma(x)$ and solve equations (1), (6), (7) and (8) for a new distribution of p, v, T_a, $\bar{\sigma}$ and L. We note, following Johannesen, that this second approximation is a solution of the equations governing the steady diabatic flow of a perfect gas with constant specific heats. The energy equation may be written as

$$Cp_a(T_a)_0 + q = Cp_a T_a + \tfrac{1}{2}v^2, \tag{9}$$

where

$$q = (\bar{\sigma}_0 - \sigma).$$

Thus the non-equilibrium nozzle flow of a real gas may be treated as a perfect gas flow with heat addition $q(x)$ equal to the reduction in the energy stored in the vibrational modes of a real gas, $\bar{\sigma}_0 - \sigma(x)$. Such perfect gas flows with area change and heat transfer are treated in many standard text-books, e.g. Shapiro

(1953) but again a step-by-step procedure is needed and the process needs care. The two limiting cases of equation (9) are worth discussing.

(*a*) Zero relaxation time, i.e. complete thermal equilibrium $\sigma = \bar{\sigma}$. The real gas flow is then isentropic. Flow properties are readily available from tables and those prepared by Erickson & Creekmore (1960) have been used in table 2 of this note.

(*b*) Infinite relaxation time, i.e. immediate freezing $\sigma = \bar{\sigma}_0$, $q = 0$. The other real gas properties are then identical with those for the isentropic flow of a perfect gas and easily calculable.

A comparison of nozzle flow exit conditions between these two limiting cases is shown in table 2.

	(*a*)	(*b*)
p_e (p.s.i.a.)	0·106	0·094
T_e (°K)	119	95·4
v_e (ft./sec)	6863	6420
a_e (ft./sec)	717	642
M_e	9·58	10·0

TABLE 2. $p_0 = 4000$ p.s.i.a., $T_0 = 2000$ °K, $A_e/A^* = 536$.

For the example chosen complete freezing of the energy in vibration reduces the pressure and temperature at exit by 11 and 20 %, respectively. The Mach number increases by 4 %.

The flow properties for the real relaxing gas will be between those calculated for cases (*a*) and (*b*). Hence if the distributions of $\sigma(x)$ calculated from equation (5*a*) starting with flow properties given by the two limiting cases are similar, then a second approximation is unnecessary, see figure 2. In practice this is the case. The correction to the first approximation is small and, remembering the assumptions in the method of analysis and the accuracy of the experimental data for τ, does not justify the labour involved.

Nozzle shape

In the calculations an axisymmetric hyperbolic nozzle geometry was used

$$\frac{A}{A^*} = 1 + \left(\frac{x \tan\theta}{r^*}\right)^2,$$

where A^* and r^* are the throat area and radius respectively, and θ is the semi-angle of the asymptote cone. Upstream of the throat θ was taken as 45°. Two downstream values were used namely $\theta = 5°$ and $\theta = 15°$. This nozzle shape approximates to the conical nozzles often used in hypersonic wind tunnels and is a convenient one to use. It is worth emphasizing that this choice of shape is not in any way essential. The simple first approximation described in § 2 can be applied to any nozzle shape, whether or not discontinuities in dA/dx exist.

3. Results

Starting with air in equilibrium at the entrance to the nozzle, departures from equilibrium are relatively small up to the throat ($T_i \simeq T_a$). Beyond the throat the vibrational temperature begins to lag further and further behind and at

some station, depending on the reservoir pressure, reservoir temperature and nozzle divergence angle, T_i freezes at a level considerably in excess of the equilibrium value. Bray (1959) has shown that a dissociating gas behaves in a similar way, the dissociation fraction freezing at some station in the nozzle.

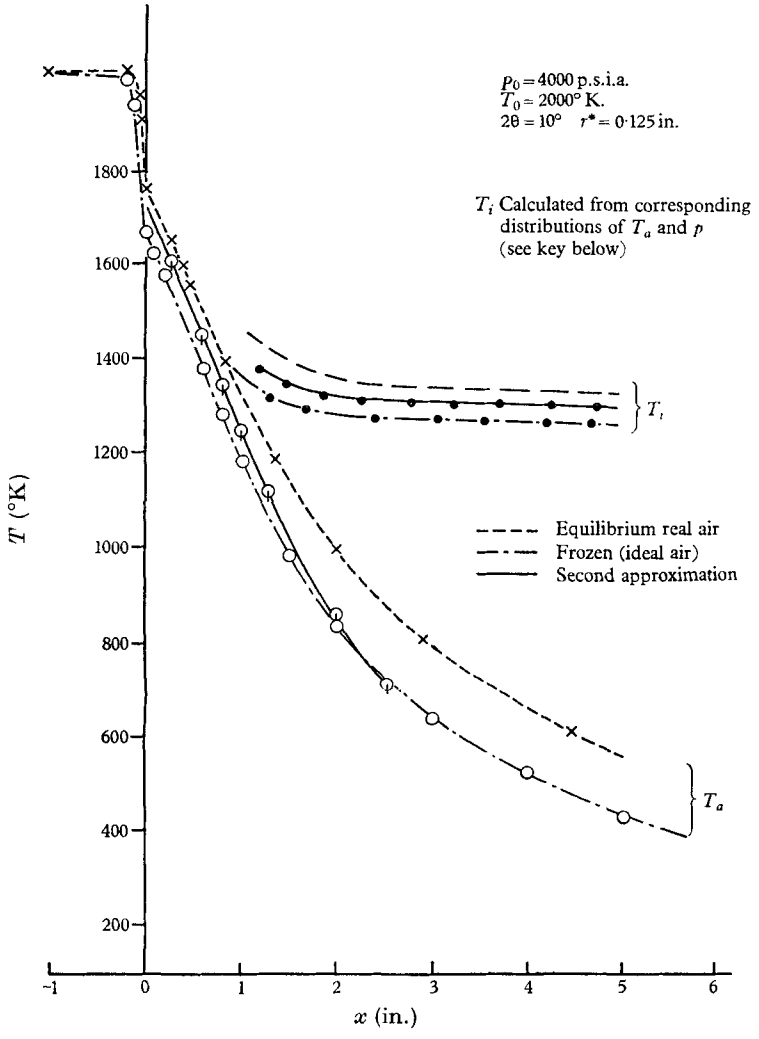

FIGURE 2. Variation of T_a and T_i along a hypersonic nozzle.

Figure 2 shows the results of a sample calculation in which equilibrium air at reservoir conditions of $p_0 = 4000$ p.s.i.a., $T_0 = 2000$ °K is expanded through a hyperbolic nozzle ($2\theta = 10°$, $r^* = 0{\cdot}125$ in.) of area ratio $A_e/A^* = 536$. For a perfect gas flow the corresponding exit Mach number is ten. The perfect gas translational temperature distribution is shown together with the corresponding first approximation to T_i.

Using this first approximation the real relaxing gas properties were calculated using the 'heat transfer to a perfect gas analogy' described in § 2. It will be noted

that initially T_a follows the real gas equilibrium values, then as the vibrational energy is 'frozen out' the translational temperature moves on to the perfect gas (i.e. frozen) curve. The second approximation to T_i is also plotted and does not differ greatly from the first approximation which has been used in compiling table 3.

	T_0 (°K)	1000			2000			3000		
2θ	p_0 (p.s.i.a.)	T_F (°K)	T_F/T_0	x_F/r^*	T_F (°K)	T_F/T_0	x_F/r^*	T_F (°K)	T_F/T_0	x_F/r^*
10°	1000	912	0·912	16	1515	0·757	20	1908	0·636	22·4
	2000	850	0·85	23	1380	0·690	28	1752	0·584	30·0
	4000	770	0·77	32	1272	0·636	32·8	1612	0·537	38·8
30°	1000	955	0·955	3·04	1712	0·856	3·6	2140	0·713	4·88
	2000	922	0·922	4·40	1577	0·788	4·90	1995	0·655	6·53
	4000	872	0·872	6·0	1450	0·725	6·40	1853	0·618	7·80

TABLE 3. Properties of relaxing gas, using first approximation. $r^* = \frac{1}{8}$ in.

4. Discussion

Figure 1 shows that the vibrational relaxation time is least when pressure and temperature are high. One expects then, for a given size and shape of nozzle, the departures from thermal equilibrium to be least when the reservoir pressure and temperature are greatest.

Table 3 and figure 3 confirm this point but it is interesting to note that in every case considered, the vibrational temperature freezes at above 50 % of the reservoir temperature and for the lower values of T_0 and p_0 the ratio T_F/T_0 reaches 90 %, freezing being complete just downstream of the nozzle throat. The point x_F has been defined as the station downstream of which T_i falls by only 1 % before the exit $A_e/A^* = 536$ is reached.

It is apparent then that for equilibrium flow throughout a hypersonic nozzle the stagnation conditions would have to be large and the divergence angle small, i.e. the nozzle very long. Larger values of T_0 are not used here since for air, oxygen dissociation becomes increasingly important above 3000 °K.

The rate equation (5) may be written in non-dimensional form

$$L' d\sigma'/d\xi = \bar{\sigma}' - \sigma', \tag{5b}$$

where $\sigma' = \sigma/\bar{\sigma}_0$, $\bar{\sigma}' = \bar{\sigma}/\bar{\sigma}_0$, $\xi = x/r^*$ and $L' = L/r^*$. Now

$$L' = \frac{v\tau}{r^*} = \frac{v(\tau p)}{p_0 r^*}\frac{p_0}{p},$$

where τp is a function of temperature only (see figure 1). If the shape of the nozzle (θ) and the reservoir temperature are specified then v, τp, $\bar{\sigma}'$ and p_0/p are all functions of ξ, and $p_0 r^*$ is a similarity parameter. The values quoted in table 2 for $p_0 = 2000$ p.s.i.a. and $r^* = \frac{1}{8}$ in. hold equally well for $p_0 = 1000$ p.s.i.a., $r^* = \frac{1}{4}$ in., and $p_0 = 4000$ p.s.i.a., $r^* = \frac{1}{16}$ in., etc. The larger the value of $p_0 r^*$

the smaller the departure from equilibrium; thus the actual nozzle size, as well as the shape and the reservoir conditions, is important.

The controlling factor for vibrational equilibrium is the way in which the relaxation length L varies with position. Differentiating equation (5*b*) gives

$$L'\frac{d^2\sigma'}{d\xi^2}+\frac{dL'}{d\xi}\frac{d\sigma'}{d\xi}=\frac{d\bar{\sigma}'}{d\xi}-\frac{d\sigma'}{d\xi}. \tag{5c}$$

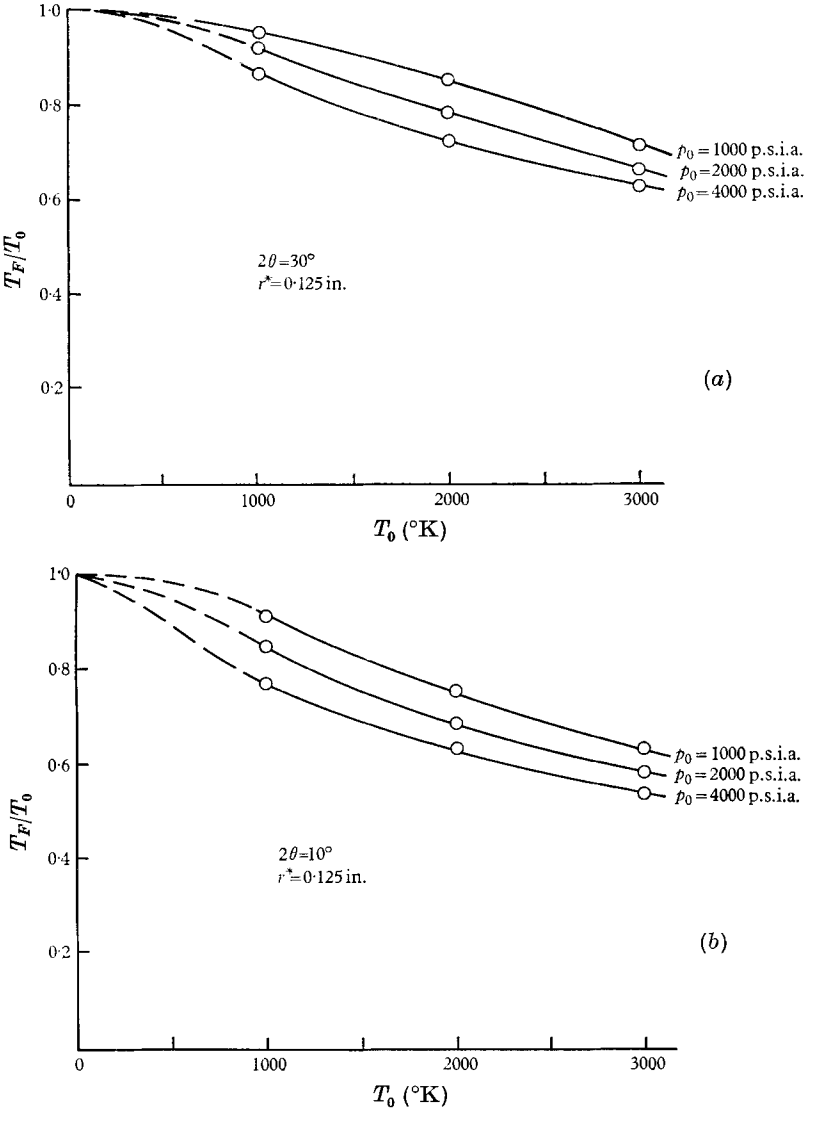

FIGURE 3. (*a*) Variation of T_F with P_0 and T_0, $2\theta = 30°$;
(*b*) variation of T_F with P_0 and T_0, $2\theta = 10°$.

The flow is assumed to be in equilibrium at nozzle entry ($x = -b$, $\xi = -b/r^*$) so that $\sigma' = \bar{\sigma}' = 1$ and $L' = 0$. Moving downstream through the nozzle the temperature and vibrational energy fall and the relaxation time increases, i.e. as

$\xi \to \infty$, $L' \to \infty$ and $\bar{\sigma}' \to 0$. Applying an order of magnitude analysis shows that if $dL'/d\xi \ll 1$ then the flow will remain in equilibrium,

$$d\bar{\sigma}'/d\xi = d\sigma'/d\xi.$$

This is because for negative ξ, $L' \ll 1$; for large positive ξ, $L' > 1$ but $d^2\sigma'/d\xi^2 \to 0$. Hence for $dL'/d\xi \ll 1$, the left-hand side of (5*c*) may be neglected and

$$d\bar{\sigma}'/d\xi \simeq d\sigma'/d\xi.$$

If, however, $dL'/d\xi \gg 1$, the flow will freeze and remain frozen i.e. $d\sigma'/d\xi \to 0$. This can be demonstrated by dividing equation (5*c*) through by $dL'/d\xi$; we note that the term $L'd^2\sigma'/d\xi^2$ does not grow large despite L' tending to infinity for large ξ since $d^2\sigma'/d\xi^2$ is everywhere small and $\to 0$ for $L' \gg 1$.

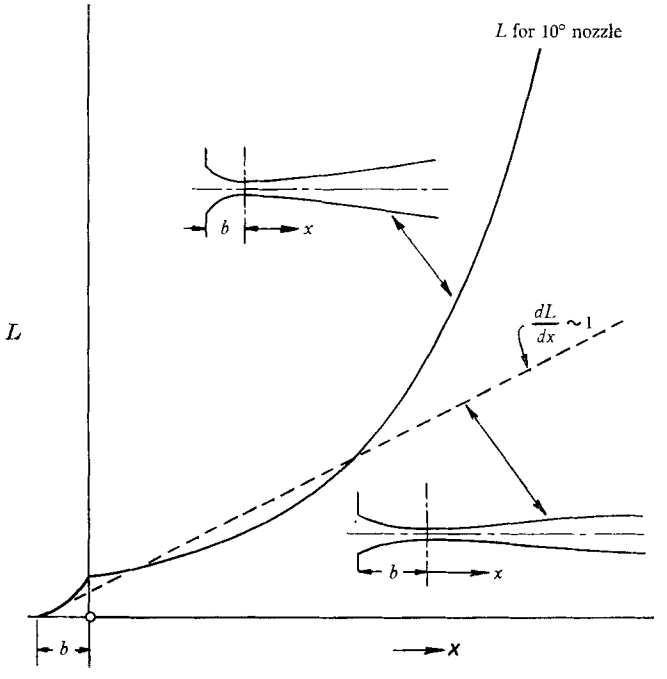

FIGURE 4. Variation of vibrational relaxation length along the nozzle (not to scale).

If $dL'/d\xi$ is $O(1)$ then $d\bar{\sigma}'/d\xi$ and $d\sigma'/d\xi$ will be of the same order, and the flow is somewhere between equilibrium and frozen. Numerical calculations show that if $dL'/d\xi = 1$ the flow is reasonably close to equilibrium.

A qualitative idea of the nozzle length (X) and nozzle shape needed to avoid vibrational non-equilibrium can be found by putting $dL'/d\xi \sim O(1)$ throughout the nozzle. Integration yields $X \sim O(L_{\text{exit}})$, i.e. $O(100\,\text{ft.})$ for the conditions of table 3. A plot of L' against (A/A^*) gives values of $d(A/A^*)/d\xi$ needed to keep $dL'/d\xi \sim O(1)$. Figure 4 shows the variation of L with x for the 10° nozzle used here. dL/dx is large just before the throat, small through the throat region and then increasingly large downstream. The nozzle shape needed to keep $dL/dx \sim O(1)$ is also sketched.

Since the method of finding T_F given in § 2.4 is quick and simple no attempt has been made to specify a numerical value of $dL/d\xi$ at which sudden freezing could be assumed to occur, in order to get a rough approximation.

5. Estimation of equilibrium static temperature from S.L.R. measurements of T_i

The results of this work show that for the hyperbolic nozzles considered, T_i and T_a are only similar over a very limited Mach number range ($0 < M < 1{\cdot}5$) and this with the proviso that p_0 and T_0 are large. Further expansion leads to an increasing divergence between T_i and T_a. The S.L.R. method can therefore only indicate T_a over the first part of a hypersonic nozzle. It can, however, give a clear indication of frozen flow downstream.

6. Estimation of equilibrium stagnation temperature from S.L.R. measurements of T_i

Measurements of the vibrational temperature can be made at the stagnation point of a blunt body placed in the supersonic or hypersonic air stream. The vibrational energy just ahead of the bow shock wave formed in front of the model, is calculated as already described ($\sigma = \sigma_1$). The vibrational energy at the stagnation point (σ_0) is then estimated assuming that the pressure and translational temperature T_a are constant in the region between the bow shock and the body surface. This means that $\bar{\sigma}$ and L are constants within the stand-off distance, $x_1 < x < x_1 + \delta$, and the rate equation may be integrated directly in this region to give

$$\sigma = A \exp(-x/L) + \bar{\sigma}, \tag{10}$$

where A is a constant. Using the boundary conditions $\sigma = \sigma_1$ at $x = x_1$, $\sigma = \sigma_0$ and $\bar{\sigma} = \bar{\sigma}_0$ at $x = x_1 + \delta$, equation (10) becomes

$$\sigma_0 = \bar{\sigma}_0 - (\bar{\sigma}_0 - \sigma_1) \exp\{-\delta/L(1+\mu)\}, \tag{11}$$

where μ is a constant, equal to $\frac{2}{7}$ for a diatomic gas, which Blythe (1961) has shown to be a necessary modification when applying the linear form of the rate equation through strong shocks. This modification has been used in preparing table 4. Equation (11) shows that only in two particular cases will σ_0, and hence the vibrational temperature measured, T_{i0}, equal the equilibrium stagnation values, $\bar{\sigma}_0$ and T_0. Either the relaxation length associated with conditions downstream of the bow shock must be much smaller than the stand-off distance, i.e. $\delta/L \gg 1$, or σ must be so close to $\bar{\sigma}_0$ already that recovery is achieved rapidly. The latter condition is possible when freezing of the vibrational energy occurs upstream of the nozzle throat.

Table 4 gives the results of calculations made to indicate the (vibrational) stagnation temperature, T_{i0}, that the S.L.R. method would measure at various points along the axis of a hypersonic nozzle. It has been assumed that, in order to produce stagnation conditions, a flat disk of area equal to 5 % of the local nozzle area is placed normal to the air stream at the various axial stations. In table 4 values of x are chosen such that the Mach number, M, increases from 4 to

12 so that the nozzle radius and hence the disk diameter increase by a factor of 10. A similar increase in the bow shock stand-off distance from the disk occurs since at high Mach numbers δ is almost directly proportional to disk diameter and independent of M. However, the relaxation length increases one hundred times over the chosen range of x so that δ/L decreases and the difference between the equilibrium stagnation temperature and the vibrational temperature measured by the S.L.R. technique becomes increasingly large.

Mach number M	4	6	8	10	12
Area ratio A/A^*	10·7	53·2	190	536	1150
Stagnation pressure p_0 (p.s.i.a.)	555	119	34	12	5·2
Mean velocity between shock and body (disk) (ft./sec)	640	595	578	569	565
Relaxation time τ (μs)	2·6	11·9	41·7	116	272
Relaxation length L (in.)	0·019	0·085	0·289	0·729	1·85
Stand-off distance δ (in.)	0·052	0·108	0·200	0·33	0·48
δ/L	2·68	1·27	0·69	0·42	0·26
σ_1 (cal./mol.)	575	570	570	570	570
Vibrational temperature at the stagnation point T_{i0} (°K)	1980	1875	1727	1600	1495
'Error' in equilibrium stagnation temperature $T_0 - T_{i0}$ (°K)	20	125	273	400	505

TABLE 4. $p_0 = 4000$ p.s.i.a., $T_0 = 2000$ °K, $r^* = \frac{1}{8}$ in., $2\theta = 10°$.

7. Conclusions

Freezing of the vibrational energy is likely to occur in hypersonic nozzles. As freezing occurs so the nozzle flow properties will diverge from the real gas equilibrium flow values. Near the nozzle exit, the error in using equilibrium values of pressure temperature and Mach number, is important.

An approximate measure of the vibrational temperature distribution may be readily calculated assuming perfect gas values for pressure and temperature (hence σ and L) plus the linear form of the rate equation.

Large corrections, to (vibrational) temperatures measured using the S.L.R. technique, may be needed when estimating either the static or the stagnation equilibrium values. Such corrections may be reduced by lowering the flow Mach number.

The authors wish to thank Prof. A. G. Gaydon for his critical interest in the work and to thank Dr I. R. Hurle, in particular, for his help and advice.

REFERENCES

BETHE, H. A. & TELLER, E. 1940 Deviations from thermal equilibrium in shock waves. *Aberdeen Proving Ground, Ballistic Research Laboratories Report* X-117.

BLACKMAN, V. H. 1956 *J. Fluid Mech.* **1**, 61.

BLYTHE, P. A. 1961 *J. Fluid Mech.* **10**, 33.

BRAY, K. N. C. 1959 *J. Fluid Mech.* **6**, 1.

Byron, S. R. 1959 *J. Chem. Phys.* **30**, 1380.

Clouston, J. G., Gaydon, A. G. & Glass, I. I. 1958 *Proc. Roy. Soc.* A, **248**, 429.

Cottrell, T. L. & McCoubrey, J. C. 1961 *Molecular Energy Transfer in Gases.* London: Butterworth and Co.

Dickens, B. G. & Ripamonti, A. 1961 *Trans. Faraday Soc.* **57**, 735.

Erickson, W. D. & Creekmore, H. S. 1960 A study of equilibrium real gas effects in hypersonic air nozzles, including charts of thermodynamic properties for equilibrium air. *Nat. Aero. Space Agency:* Tech. Note D-231.

Gaydon, A. G. & Hurle, I. 1960 *8th International Symposium on Combustion* (*Pasadena*). (In the Press.)

Henry, P. S. 1932 *Nature, Lond.*, **129**, 200.

Hilsenrath, J., Beckett, C. W. *et al.* 1955 Tables of Thermodynamic Properties of Gases. *Nat. Bur. Stand.* (*Wash.*), Circular 564.

Huber, P. W. & Kantrowitz, A. 1947 *J. Chem. Phys.* **15**, 275.

Johannesen, N. H. 1961 *J. Fluid Mech.* **10**, 25.

Knötzel, H. & Knötzel, L. 1948 *Ann. Physik*, **2**, 393.

Lukasik, S. J. & Young, J. E. 1957 *J. Chem. Phys.* **27**, 1149.

Sedney, R. 1961 *J. Aerospace Sci.* **28**, 189.

Shapiro, A. H. 1953 *The Dynamics and Thermodynamics of Compressible Fluid Flow.* New York: Ronald Press.

Stollery, J. L. 1961 *Nature, Lond.*, **190**, 778.

Tanczos, F. I. 1956 *J. Chem. Phys.* **25**, 439.

Wood, W. W. & Kirkwood, J. G. 1957 *J. Appl. Phys.* **28**, 395.